



CHAPTER IV

n-OCTANE AROMATIZATION OVER Pt SUPPORTED ON DIFFERENT PARTICLE SIZES*

4.1 Abstract

The effects of varying zeolite particle size in the n-octane aromatization over Pt/KL have been studied on a series of catalysts. Various KL zeolites were synthesized via microwave-hydrothermal treatment, which allows for a good control of crystallite morphology. Zeolites with different particle sizes were prepared by varying ageing time (17-24 h), amount of barium (0-445 ppm), and seeding (0-8 wt%). The results showed that the higher ageing time resulted in smaller zeolite particle size, whereas, the addition of barium resulted in larger particle size. Moreover, the addition of seeding reduces the particle size from 1.47 to 0.94 μm . Pt supported on different zeolite catalysts (Pt/KL) were prepared by vapor phase impregnation (VPI). The fresh catalysts were characterized by DRIFTS of adsorbed CO and volumetric hydrogen chemisorption. The results indicated that Pt clusters are well-dispersed inside the zeolite channel in all the catalysts prepared. The aromatization of n-octane was tested on the different catalysts at 500°C and atmospheric pressure. It was found that the catalytic activity of all catalysts dropped rapidly after about 200 min on stream due to coke plugging inside the pore of KL zeolite. It was also observed that less ethylbenzene (EB) and o-xylene (OX) were obtained as the conversion increased because both EB and OX are converted to smaller molecules such as benzene, toluene, etc. by secondary hydrogenolysis. Furthermore, the EB/OX ratio increased with zeolite particle size due to an enhanced preferential conversion of the larger OX molecules compared to the narrower EB as their path through the pores are restricted.

Keywords: n-octane aromatization, zeolite, microwave-hydrothermal treatment technique

*Published in Chemical Engineering Communications (2007), 194, 946-961.

4.2 Introduction

The aromatization of n-alkane is an important reaction to obtain high value-added products from a naphtha feedstock that is abundant in refinery operations. This reaction can be used in many industrial applications and can be carried out with either bifunctional (acid-metal) or monofunctional (only-metal) catalysts. The advantage of using monofunctional catalysts is that they are not active for isomerization paths, which typically occur on the bifunctional catalysts and result in lower selectivity to aromatics [1]. Platinum supported on alkaline LTL zeolite (Pt/KL) is an efficient catalyst for the dehydrocyclization of n-hexane into benzene [2-4]. However, for n-octane aromatization, Pt/KL catalysts are not as effective as for n-hexane aromatization. Although Pt/KL catalysts prepared by vapor phase impregnation (VPI) provide very high dispersion of Pt clusters that remain inside the channels of the zeolite [5-6], the selectivity for n-octane aromatization is still low and quickly drops after a few hours on stream [7]. The product distribution shows benzene and toluene as major aromatics products, with small quantities of ethylbenzene (EB) and o-xylene (OX), which are the only two expected products from a direct six-membered ring closure. The pore size of the KL zeolite is 0.71 nm, that is, larger than the critical diameter of EB but smaller than that of OX, thus OX diffuses through the zeolite crystals much more slowly than EB. As a result, OX is preferentially converted to benzene and toluene before escaping from the pore of zeolite. In our previous study [7], it was proposed that the pore length of the zeolite should have a great impact on product distribution and catalyst life.

The idea of short channel KL zeolite has been previously discussed by Treacy [8] to minimize the problem of Pt entombment due to metal agglomeration and coking. Furthermore, the zeolite with small crystallite size provides advantages over zeolites with large crystallite size by enhancing the ratio of surface area to mass. These advantages are higher diffusion rates and a lower rate of deactivation by pore plugging [9]. Many researchers have focused on synthesis of KL zeolites by conventional hydrothermal treatment [10-14]. However, in the hydrothermal treatment, the heat transfer by both convection and conduction results in a slow temperature increase, which lengthens the crystallization time. The use of

microwave radiation has been found to be advantageous in the production of microporous crystalline materials in comparison to the conventional method. The volumetric heat generated by microwaves results in a more homogeneous nucleation process and yields crystalline materials in shorter times than the conventional method [15]. Furthermore, it is a clean and economical heating system [16-17]. To reduce the crystallite size of zeolite, crystallization conditions and composition-dependent parameters were investigated [18]. It was found that the ageing process can reduce the size of zeolite crystals in the final product [19-20]. Incorporation of colloidal L zeolite seeds into the gel before crystallization can also reduce the crystallite size [19].

In this contribution, we attempt to evaluate the effects of varying the zeolite crystallite size on the n-octane aromatization over Pt/KL catalysts. First, several KL zeolites were synthesized by using microwave hydrothermal treatment. The effects of synthesis conditions including ageing time, amount of barium, and seeding on crystallite size of zeolite KL were investigated. The synthesized KL zeolites were characterized using X-ray diffraction (XRD), nitrogen adsorption (BET), scanning electron microscopy (SEM), X-ray fluorescence (XRF), Fourier transform infrared spectroscopy (FT-IR), and dynamic light scattering spectrometry (DLS). Pt supported on the synthesized KL zeolites were prepared by vapor phase impregnation (VPI) and tested for their activity and selectivity of n-octane aromatization at 500°C and atmospheric pressure. This impregnation method has been shown to be the most effective to maximize selectivity to benzene from n-hexane [5-7]. The fresh catalysts were characterized by means of FTIR of adsorbed CO that provides information about the location of the Pt particles and hydrogen chemisorption that quantifies the metal dispersion. Temperature programmed oxidation (TPO) was used to analyze the amount and nature of coke deposited on the catalysts.

4.3 Experimental

4.3.1 Materials

n-Octane (C₈H₁₈) of min. 99% purity was obtained from Merck. The commercial K-LTL zeolite (HSZ-500, SiO₂/Al₂O₃ = 6, surface area =280 m²/g) was obtained from Tosoh, Japan. Platinum (II) acetylacetonate ([CH₃COCH=(CO-)CH₃]₂Pt) was obtained from Alfa Aesar. Colloidal silica (40wt% suspension) was obtained from Aldrich. Potassium hydroxide (KOH) and Barium hydroxide (Ba(OH)₂) were supplied by Carlo Erba. Aluminium hydroxide (Al(OH)₃) of 99.8% purity was acquired from Merck.

4.3.2 Synthesis of KL Zeolites

The KL zeolites were synthesized from a mixture of silicate and potassium aluminate solutions to attain the following composition: 2.65K₂O: 0.0032BaO: 0.5Al₂O₃: 10SiO₂: 159H₂O. The potassium aluminate solution was prepared by dissolving 2.64 g of Al(OH)₃ in the 8.15 M of KOH solution. The silicate solution was prepared by mixing colloidal silica with 2.8 mM of Ba(OH)₂ solution and stirring for 15 min. The silicate and aluminate solutions were then mixed and stirred vigorously by a mechanical stirrer for different periods of ageing time at ambient temperature. After that, the gel mixture was transferred to a microwave vessel and heated using a MARS5 microwave machine up to 170°C within 2 minutes and maintained at that temperature for 15-50 h. As a way of comparison, an L zeolite synthesized in a conventional manner was aged for 24 h and transferred to a 250 ml Teflon-lined autoclave that was then placed in an oven at 170°C and held at that temperature for 96 h. Moreover, the effects of adding barium (0-445 ppm) and seeding (0-8 wt%) were studied. The resultant material was washed with deionized water until a pH of 10 was reached. Then, it was centrifuged to separate the solid phase from the solution. The solid product was dried in an oven at 110°C overnight and then calcined at 500°C in flowing air. The synthesized zeolites are named by their synthesized conditions and compositions as listed in Table 4.1.

Table 4.1 List of zeolites and their characteristics

Zeolites*	Ageing time (h)	Cryst. time (h)	Amount of Ba (ppm)	Amount of seeding (wt%)	Particle size (μm)	Surface area (m^2/g)	Pore volume (cm^3/g)	Si/Al ratio
Commercial KL	n/a	n/a	n/a	n/a	0.53	302	0.206	3.00
A17/C30/B1	17	30	115	0	1.81	124	0.092	3.60
A24/C30/B1	24	30	115	0	1.47	144	0.093	3.30
A30/C30/B1	30	30	115	0	1.51	n/a	n/a	3.27
A24/C30/B2	24	30	230	0	1.63	147	0.122	3.37
A24/C30/B3	24	30	345	0	2.07	156	0.124	3.27
A24/C25/B1/S2	24	25	115	2	0.99	239	0.158	n/a
A24/C25/B1/S5	24	25	115	5	0.94	228	0.171	2.93
A24/C25/B1/S8	24	25	115	8	1.14	136	0.100	n/a
A24/C96/B1**	24	96	115	0	1.14	170	0.112	3.20

*Axx represents the ageing time of xx h., Cxx represents the crystallization time of h., Bx represents the amount of barium with 115, 230 and 345 ppm where x=1,2 and 3, respectively, and Sx represents the seeding used of x wt%

**Synthesized by using conventional hydrothermal treatment

4.3.3 Characterization of the Synthesized KL Zeolites

The structures of synthesized KL zeolites were evaluated using a Rigaku X-ray diffractometer, with Cu-K line as incident radiation, and a filter at a scanning rate of 5°/s. The Si/Al ratio was measured using an SRS 3400 Bruker X-ray fluorescence spectroscope, with 99.8% boric acid as binder. The crystal morphology was investigated using a JEOL 5200-2AE scanning electron microscope. A Malvern 4700 DLS spectrophotometer equipped with Ar-ion laser as a light source was used to determine the average particle size. The detector was fixed at 60° with respect to incident beam direction. The photomultiplier aperture used was 150 µm. Nitrogen adsorption was employed to analyze the surface area and pore volume of synthesized KL zeolites. The adsorption isotherms were collected at 77K using a Thermo Finnigan sorptomatic modeled 1100 series.

4.3.4 Catalyst Preparation

The various Pt/KL catalysts investigated were prepared by vapor phase impregnation (VPI) of the different L zeolites. Prior to impregnation, the zeolite support was dried in an oven at 110°C overnight and calcined at 500 °C in flowing dry air of 100 cm³/min.g for 5 h. The Pt/KL catalysts were prepared by physical mixing a weighed amount of platinum (II) acetylacetonate (Pt(acac)₂) with a proper amount of dry zeolite support under nitrogen atmosphere. The mixture was then loaded in a tubular reactor before being subject to a helium flow of 5 cm³/min.g. The reactor was gradually ramped to 40°C and held for 3 h, and ramped again to 60°C and held for 1 h. After that, it was further ramped to 115°C at which the mixture was held for 1 h to sublime the Pt(acac)₂. After being cooled down to room temperature, it was ramped to 350°C in flowing air and held for 2 h to decompose the platinum precursor. The actual metal content was analyzed by a Varian modeled SpectraA-300 atomic absorption spectroscopy.

4.3.5 n-Octane Aromatization Activity of the Catalysts

The catalytic activity studies were conducted at atmospheric pressure in a 0.5–inch glass tube inserted with an internal K-type thermocouple for temperature measurement and control. The reactor was a single-pass and continuous-flow type. Two hundred milligrams of the catalysts were used in each

run. Prior to reaction, the catalyst was slowly ramped in flowing H₂ for 2 h up to 500°C and in-situ reduced at that temperature for 1 h. *n*-Octane was introduced to the system using a syringe pump. In all experiments, the hydrogen-to-*n*-octane molar ratio was maintained at 6:1. The products were analyzed using a Shimadzu 17A-GC equipped with an HP-PLOT/Al₂O₃ “S” deactivated capillary column. The GC column temperature was programmed to obtain an adequate separation of the products. The GC oven temperature was first kept constant at 40°C for 10 min and then it was linearly ramped with a heating rate of 5 °C/min to 195°C and held for 30 min.

4.3.6 Catalyst Characterization

4.3.6.1 *Diffuse Reflectance Infrared Fourier Transform Spectroscopy (DRIFTS) of Adsorbed CO*

The fresh Pt/commercial KL and Pt/synthesized KL catalysts were characterized by DRIFTS using CO as a probe in a Bruker Equinox 55 spectrometer equipped with an MCT detector. Experiments were performed in a diffuse reflectance cell from Harrick Scientific typed HVC-DR2, with ZnSe windows. For each IR spectrum, a background was collected on the sample reduced in situ under a flow of H₂ at 300°C for 1 h and purged in He for 30 min at ambient temperature. Then, a flow of 5%CO in He was passed through the sample for 30 min, followed by a purge in He flow for 30 min. After such a treatment, the spectrum of adsorbed CO was collected.

4.3.6.2 *Hydrogen Chemisorption*

Hydrogen uptake and degree of dispersion were determined by using a pulse technique (Thermo Finnigan modeled TPDRO 1100). Prior to the pulse chemisorption, the sample was reduced in H₂ atmosphere at 500°C for 1 h. Consecutively, it was purged with N₂ at 500°C for 30 min and cooled down to 50°C in flowing N₂. H₂ pulses (purged H₂, 0.4 ml) were injected onto the sample at 50°C until the saturation was observed.

4.3.6.3 *Temperature Programmed Desorption (TPD) of Isopropylamine*

The acidity of catalyst prepared was tested by the amine TPD technique developed by Gorte and co-workers [21]. The test was conducted in a 1/4 in. quartz reactor. First, 30 mg of sample was pretreated at 500 °C in a flow of He for 1 h. After the pretreatment, the sample was cooled in He to room temperature and then 30 µl of isopropylamine was injected over the sample. After removing the excess of isopropylamine by flowing He overnight, the sample was linearly heated to 700 °C at a heating rate of 10 °C/min. Masses 44, 41, and 17 were monitored to determine the evolution of isopropylamine, propylene, and ammonia, respectively. The amount of desorbed propylene was calibrated with 5 ml pulses of 2% propylene in He.

4.3.6.4 Temperature Programmed Oxidation (TPO)

This technique was employed to analyze the amount and characteristics of coke formation on the spent catalysts. TPO of the spent catalysts was performed in a continuous flow gas of 2% O₂ in He and the temperature was linearly increased with a heating rate of 12°C/min. The oxidation reaction was conducted in a 1/4" quartz fixed-bed reactor. The spent catalyst was dried at 110°C overnight. Thirty milligrams of dried sample were placed in between the layers of quartz wool. The sample was flushed by flowing 2% O₂ in He for 30 min before the TPO was performed. CO₂ produced by the oxidation of coke species was further converted to methane using a methanizer filled with 15% Ni/Al₂O₃ and operated at 400°C. The methane was analyzed as a function of temperature using an FID detector.

4.4 Results and Discussion

4.4.1 Synthesis of KL Zeolites

4.4.1.1 *Effect of Ageing and Crystallization Times*

For the controlled synthesis of KL zeolites by microwave-hydrothermal treatment technique (MH), ageing times and crystallization times were systematically varied. In this way, the optimum conditions to produce crystalline KL zeolites were determined. The ageing times and crystallization times were varied in

the range of 0-30 h and 20-50 h, respectively. XRD patterns of selected synthesized zeolites are shown in Figure 4.1. Their crystallinity as functions of ageing and crystallization times is presented in Figure 4.2. It was found that when the gel was not aged, amorphous phase was observed even though the crystallization time was increased. This is because with no ageing processes, the solution does not have enough nucleation centers to induce the crystal growth [22]. Furthermore, if the gel was aged for less than 17 h, a mixture of KL zeolites, amorphous phase as well as other crystal phases, was observed. The appearance of pure crystalline KL was only detected at ageing times longer than 17 h and crystallization time of 30 h. Crystalline KL mixed with amorphous material was obtained when the crystallization times were shorter than 30 h. In contrast, other crystal phases were formed when the crystallization time was longer than 30 h as shown in Figure 4.3. In addition, it was found that to synthesize zeolite by conventional hydrothermal treatment (CH), much longer crystallization times (96 h) were needed, compared with much shorter times for microwave treatment (see Figure 4.1).

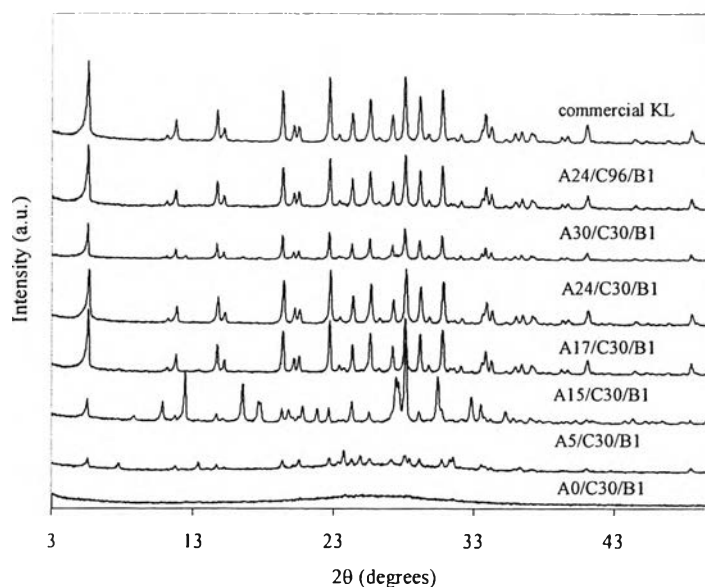


Figure 4.1 XRD patterns of synthesized KL zeolites obtained with different ageing times at crystallization temperature of 170°C and crystallization time 30 h.

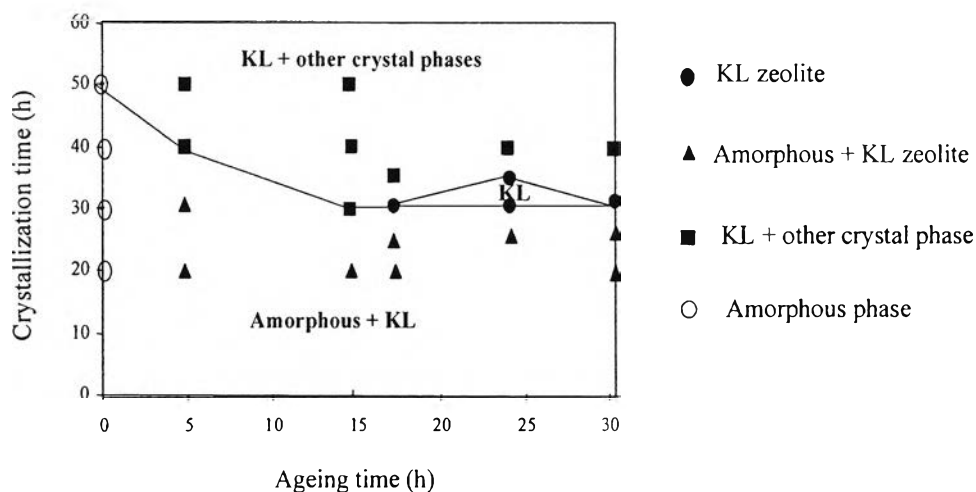


Figure 4.2 Characteristics of products obtained with various ageing and crystallization times.

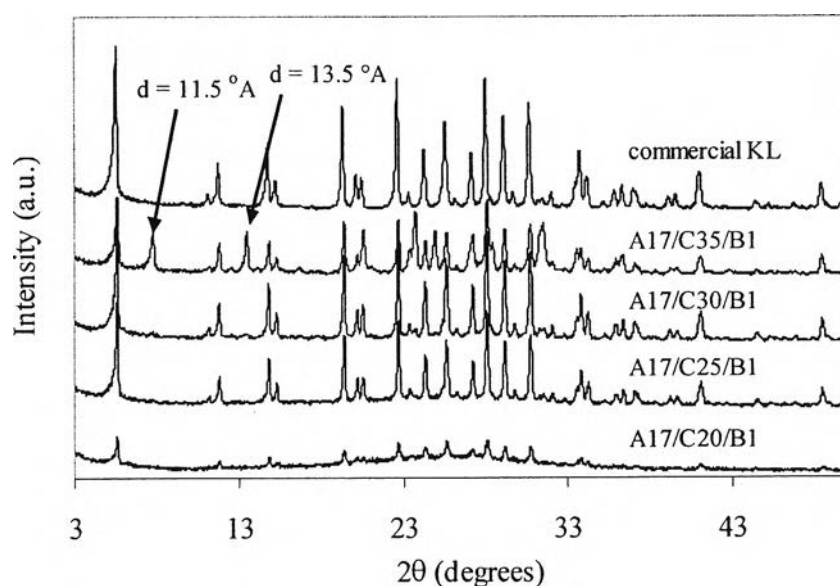


Figure 4.3 XRD pattern of synthesized KL zeolites obtained with different crystallization times at crystallization temperature of 170°C and ageing time of 17 h.

FTIR is another technique that can be used to verify the crystallinity of the synthesized zeolites. Spectra of the synthesized zeolites prepared with different ageing times and compositions are compared in Figure 4.4 to commercial KL zeolite. As previously reported [23], an absorption band centered at

620 cm^{-1} is characteristic of crystalline KL, such results are in good agreement with those obtained by XRD (Figure 4.1).

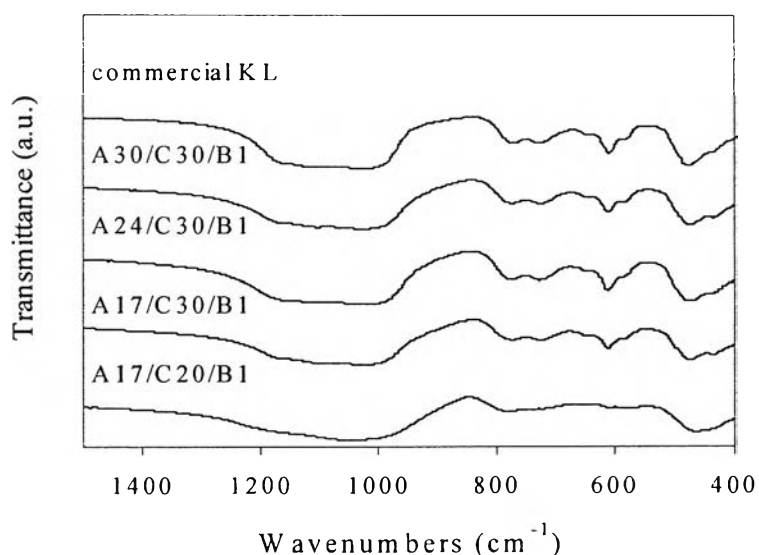


Figure 4.4 FTIR spectra of synthesized KL zeolites obtained with different ageing times at crystallization time of 33 h compared to amorphous KL zeolite.

The Si/Al ratio, particle size, surface area, and pore volume of all the synthesized and commercial KL zeolites were determined by XRF, DLS, and BET, respectively. The results are listed in Table 4.1. It was found that under the same conditions, the zeolites obtained with 24 h ageing time resulted in smaller particle size ($1.47\ \mu\text{m}$) than the one obtained with 17 h ageing time ($1.81\ \mu\text{m}$). This result is in good agreement with a previous study done by Ertl et al. [24]. They reported that the zeolite prepared with longer ageing time resulted in smaller crystal size because at longer ageing time, the concentration of nuclei was enhanced. However, ageing times longer than 30 h did not result in further reduction of particle size. The particle sizes of synthesized zeolites are still larger by a factor of 3 compared to that of the commercial KL. Also, the surface area and pore volume of the synthesized KL zeolites are much lower than those of the commercial KL. XRF results showed that the Si/Al ratios for all synthesized KL zeolites are in between 3.2 and 3.5 while that of the commercial KL is at 3.0. SEM images of the synthesized and commercial KL zeolites are shown in Figure 4.5. It is clearly seen that the

synthesized KL zeolites are in flat-cylindrical shape whereas the commercial KL is in irregular spherical shape.

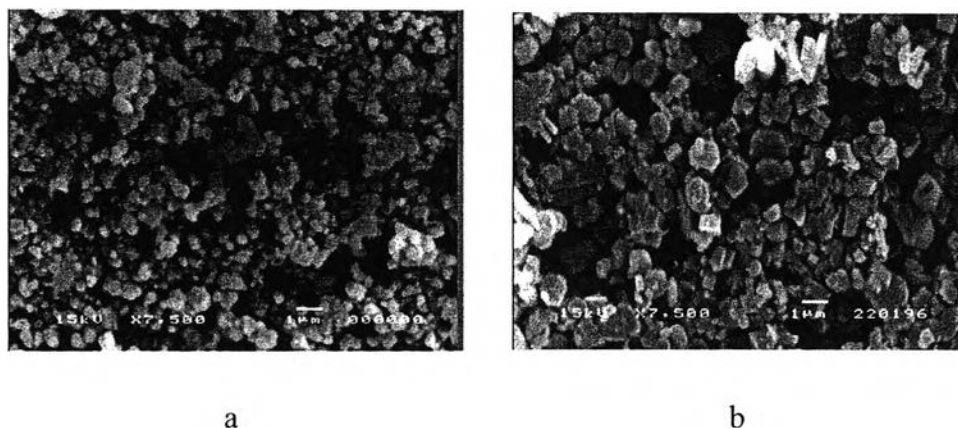


Figure 4.5 SEM images of synthesized KL zeolite crystal obtained with (a) commercial KL zeolite (b) ageing time of 24 h and crystallization time of 30 h (A24/C30/B1).

4.4.1.2 Effect of Barium

It has been reported that the formation of KL zeolite can be promoted by addition of Ba [12,13]. In this report, the effect of barium on the formation of KL zeolite was investigated by varying the amount of barium from 0 to 445 ppm. The synthesis gel was aged for 24 h and heated to 170°C for 30 h for the crystallization process. All synthesized KL zeolites were characterized by FTIR. The results shown in Figure 4.6 revealed that, without Ba, the characteristic band of KL zeolite at 620 cm^{-1} was not observed. That is, the product was amorphous aluminosilicate. However, when small amounts of barium were added, crystalline KL was obtained. In addition, it was found that a higher amount of barium resulted in a larger particle size, as shown in Table 4.1. The particle size was increased from 1.47 to 2.07 μm when the amount of barium was increased from 115 to 445 ppm. However, the surface area, pore volume, and Si/Al ratio were not significantly different among the various zeolites prepared with different amounts of Ba.

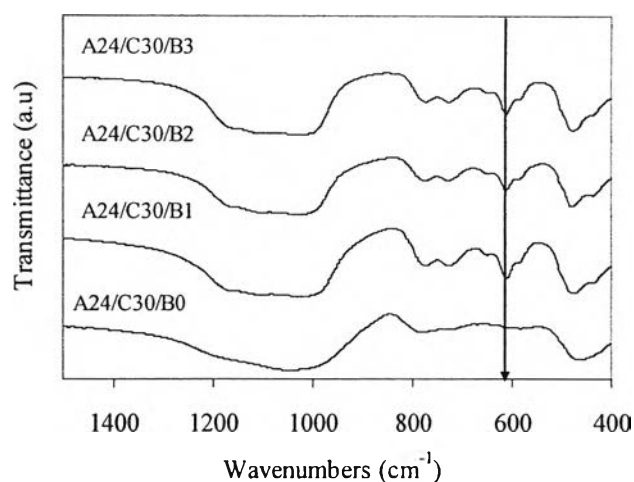


Figure 4.6 FTIR spectra of synthesized KL zeolites obtained with the different amounts of barium at ageing time of 24 h and crystallization time of 30 h.

4.4.1.3 Effect of Seeding

Seeding is a technique of adding small amounts of small particles of material to help crystallization of the synthesis gel; this is typically done just before the crystallization step to direct the crystallization process towards a desired zeolite structure. Seeding can increase the crystallization rate resulting in shorter crystallization time and also helps controlling the size of the final crystals [24]. If zeolite is formed at lower temperature and shorter crystallization time, the crystallite size obtained should be smaller [25]. Therefore, crystallization time was additional parameter that we have adjusted in this work to control the crystallite size. Here, we have used commercial KL zeolite as a seed. The amount of seed added to the mixture was varied from 0-8 wt%. The crystallization time was reduced from 30 to 25 h when seed was added. From Table 4.1, it was found that the amount of seed when ranging from 2 to 5 wt% resulted in smaller crystal as compared to other synthesized zeolites, compared to zeolites without seeding at crystallization time of 30 h, the addition of seed resulted in the reduction of the particle size from 1.47 to 0.94 μm as shown in Figure 4.7.

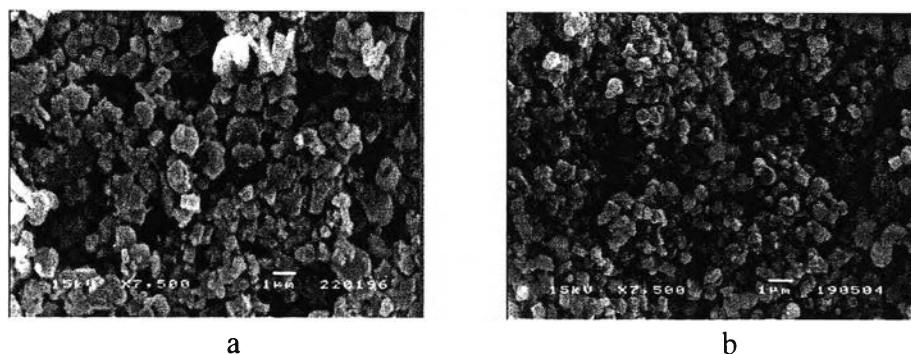


Figure 4.7 SEM images of synthesized KL zeolites obtained with (a) 0 wt% seeding at ageing time of 24 h and crystallization time of 30 h and (b) 5 wt% seeding at ageing time of 24 h and crystallization time of 25 h.

4.4.2 Characterization of the Fresh Catalysts

To study the effect of particle size on catalytic activity and selectivity for n-octane aromatization, a number of synthesized zeolites with different particle sizes were selected for preparing Pt/KL catalysts and compared with Pt/KL catalysts prepared with commercial KL zeolite (0.53 μm). As summarized in Table 4.1, the zeolite samples used to prepare catalysts were in the following: A24/C25/B1/S5 (0.94 μm), A24/C30/B1 (1.47 μm), A17/C30/B1 (1.81 μm), and A24/C30/B3 (2.07 μm), where Axx stands for ageing time in h, Cxx for crystallization time in h, Bx for the amount of Ba with 115, 230, and 345 ppm where $x=1,2,\text{and }3$, respectively; and Sx for the seeding used of x wt%; the number in parenthesis is the particle size. For the sake of simplicity, in the rest of the text the catalysts are identified only by the average particle size; i.e., Pt/KL-0.94, Pt/KL-1.47, Pt/KL-1.81, Pt/KL-2.07, and Pt/KL-0.53, respectively.

All Pt/KL catalysts were analyzed by diffuse reflectance FTIR of adsorbed CO (DRIFTS) and pulse hydrogen chemisorption techniques. As in previous studies of our group, DRIFTS has been employed to investigate the size and location of the Pt clusters in the KL zeolite [2,3,7]. A typical FTIR spectrum of CO adsorbed on Pt/KL exhibits bands in the region 2150-1900 cm^{-1} . The band below 2050 cm^{-1} represents Pt clusters located inside the channels of the L zeolite whereas

the band between 2050 cm^{-1} and 2075 cm^{-1} corresponds to larger Pt clusters located at the pore mouth of the L zeolite, and the bands above 2075 cm^{-1} represents Pt clusters located outside the L zeolite pores. DRIFTS spectra for different Pt/KL catalysts are shown in Figure 4.8. The strong absorption bands at the lower frequencies for all the catalysts in series indicate that, even though the particle sizes are different, all of the catalysts present a large fraction of small Pt clusters inside the channels of KL zeolite, and a small fraction of Pt clusters located at the pore mouth and outside of the zeolite pores.

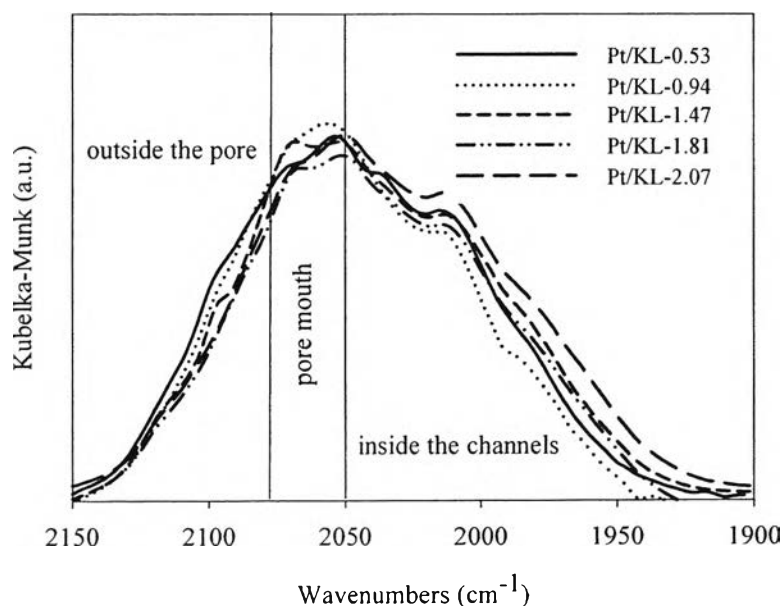


Figure 4.8 DRIFTS spectra of CO adsorbed on different particle sizes of Pt/KL catalysts.

Hydrogen chemisorption was used to determine the Pt dispersion of the fresh catalysts, after reduction at 500°C . The Pt dispersions expressed in terms of the H/Pt ratio are reported in Table 4.2. Most of the catalysts yielded H/Pt ratios higher than unity, indicating a very high state of dispersion, consistent with the formation of small Pt clusters that have a particle size diameter of less than 1 nm [26].

Table 4.2 Analysis of fresh and spent catalysts

Catalysts	Zeolite supports	Fresh catalysts		Spent catalysts
		Pt content (wt%)	H/Pt after reduction at 500°C	Coke deposited after rxn with n-octane for 550 min (wt%)
Pt/KL-0.53	Commercial KL	0.98	1.48	2.21
Pt/KL-0.94	A24/C25/B1/S5	1.06	1.12	1.35
Pt/KL-1.47	A24/C30/B1	0.94	1.17	0.76
Pt/KL-1.81	A17/C30/B1	0.96	1.15	0.83
Pt/KL-2.07	A24/C30/B3	0.94	1.04	1.26

TPD of isopropylamine was performed on selected catalysts i.e. Pt/KL-0.53, Pt/KL-1.81, Pt/KL-2.07. The result illustrates that the prepared catalysts have no residual acidity as no peak of $m/e = 44, 41, 17$ was found during the course of increasing temperature. In addition, there is high fraction of peak of $m/e=44$ which is corresponded to the unreacted isopropylamine as shown in Figure 4.9.

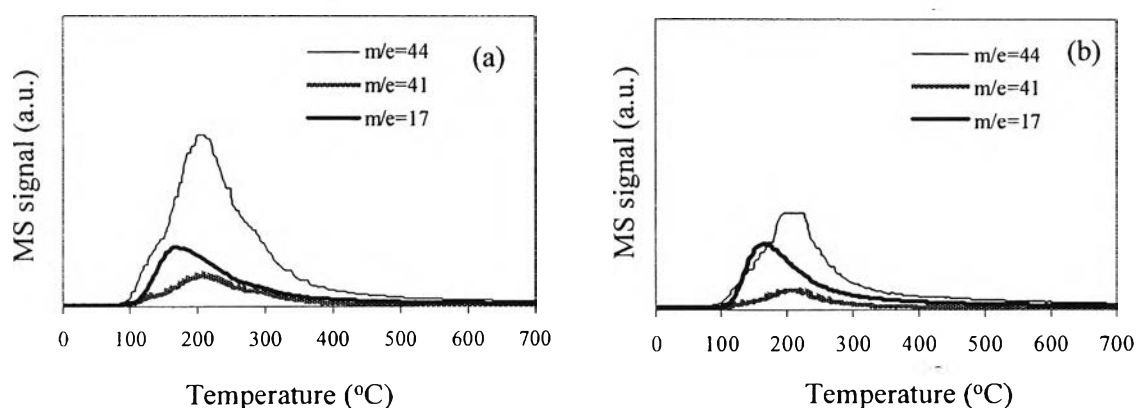


Figure 4.9 Mass spectra of TPD of isopropylamine of (a) Pt/KL-0.53 and (b) Pt/KL-2.07.

4.4.3 Catalytic Activity Measurements

The prepared Pt/KL catalysts with different zeolite particle sizes were tested for their catalytic activity and selectivity of n-octane aromatization. The conversion and selectivity to total aromatics are shown in Figures 4.10(a) and 4.10(b), respectively. After 10 min on stream, the n-octane conversions are almost 100% for all catalysts. However, these catalysts deactivated quickly during the first few hours on stream due to coke deposition that plugs the pores of the KL zeolite [8]. Regardless of their particle size, all catalysts exhibited similar selectivity towards the total aromatics. Moreover, all catalysts resulted in low C8 aromatics selectivity (ethylbenzene (EB), o-xylene (OX), m-xylene (MX), and p-xylene (PX)) when compared to the selectivity for total aromatics (see Table 4.3). The major aromatic products were benzene and toluene, which are the secondary products from hydrogenolysis of EB and OX over the Pt clusters, as has been reported in our previous work [7].

Table 4.3 Properties of various catalysts tested for n-octane aromatization after 550 min

Properties	Pt/KL-0.53	Pt/KL-0.94	Pt/KL-1.47	Pt/KL-1.81	Pt/KL-2.07
Conversion (%)	23.30	21.80	25.20	18.20	29.20
Product distribution (%)					
C1-C5	19.70	22.50	21.80	21.60	24.60
Total enes (C6-C8enes)	12.40	9.70	5.50	8.10	5.50
Total aromatics	67.90	67.8	72.70	70.20	69.90
Total aromatics (%)					
Benzene	19.00	17.90	21.3	18.20	23.90
Toluene	27.60	31.70	34.3	32.40	28.30
EB	13.90	12.70	12.4	14.90	15.20
m-p-Xylene	1.80	3.90	3.00	3.00	2.40
o-Xylene	5.50	3.90	3.00	3.00	2.40
EB/OX ratio	2.60	3.30	4.20	4.90	6.30

T 95157698

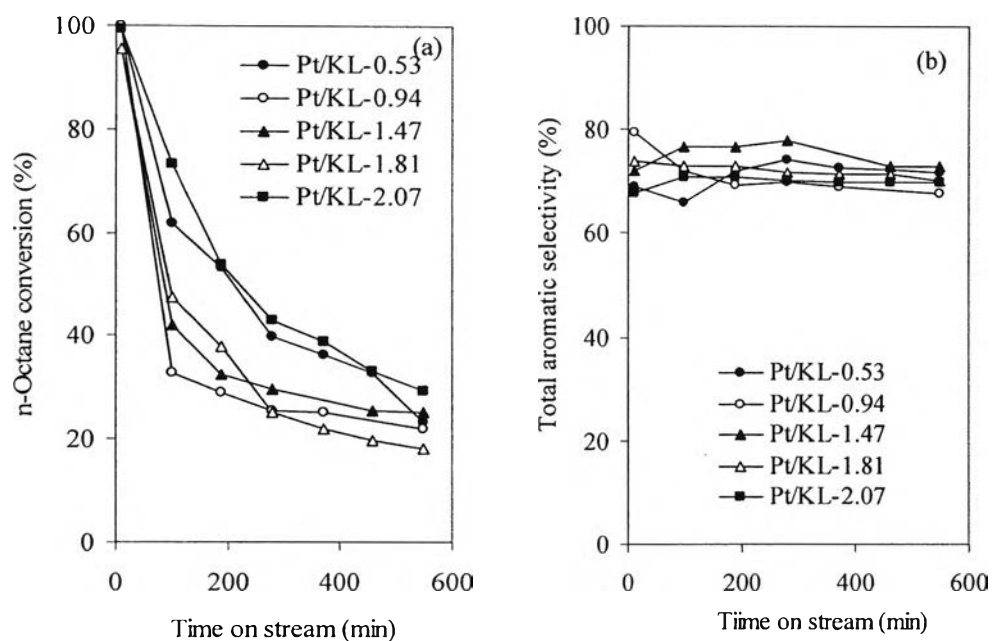


Figure 4.10 The variation of (a) n-octane conversion (b) total aromatics selectivity with time on stream of Pt/KL catalysts at 500°C, WHSV= 5 h⁻¹, and H₂/HC=6.

The EB/OX ratio is a good indicator of the importance of diffusional effects in the reaction [7]. The ratio of the primary products EB/OX is about unity from the direct aromatization on Pt surfaces, free of diffusional effects. In fact a ratio of unity is observed over nonmicroporous Pt/SiO₂ catalysts [7]. On the other hand, the EB/OX ratio becomes greater than 1 when there is pore restriction and it gets greater as the diffusional effects become more pronounced, for example by carbon deposition. Since the critical size of the OX molecule is larger than that of EB, the diffusion of OX is slower than EB and easily converted to smaller molecules such as benzene, toluene, and methane by secondary hydrogenolysis. Figure 4.11 shows the evolution of EB/OX ratio as a function of zeolite particle size. It is observed that the ratio rapidly increased with increasing particle size. It is clear that the difference in rate of diffusion out of the zeolite of EB and OX after being formed makes the slower molecule (OX) more susceptible to secondary conversion as the particle size increases than the faster molecule (EB).

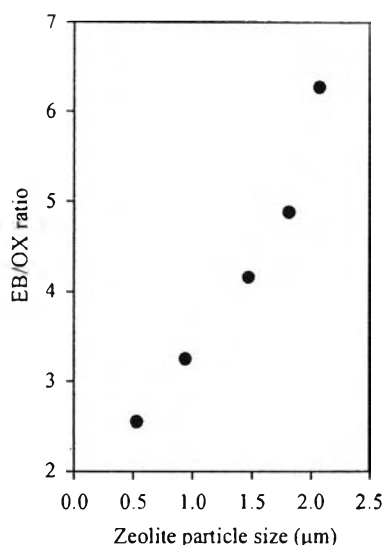


Figure 4.11 The variation of EB/OX ratio obtained from different Pt/KL catalysts at 460 min time on stream as a function of zeolite particle size. Reaction conditions: Temperature= 500°C, WHSV= 5 h⁻¹, and H₂/HC= 6.

4.4.4 Characterization of Spent Catalysts

The spent catalysts were analyzed by a temperature programmed oxidation (TPO) technique to determine the amount of coke deposited after n-octane aromatization reaction for 550 min. The results are summarized in Table 4.2. The results showed that significantly smaller amounts of coke were deposited on the Pt/synthesized KL zeolites than on the Pt/commercial KL. Moreover, the TPO profiles shown in Figure 4.12 indicate that a large fraction of the excess carbon deposited on the Pt/commercial KL was only oxidized at high temperatures. Such a high temperature band is thought to be due to carbon blocking zeolite pores [27]. The significant differences shown in TPO and in the EB/OX ratio suggest that the catalysts prepared with smaller zeolite crystallites should behave better in terms of selectivity and resistance to deactivation. It is postulated that the rate of deactivation should be much less pronounced at higher pressures, under conditions in which the presence of high partial pressures of hydrogen can help remove the coke precursors. It is possible that under such conditions, the effect of particle size will be more pronounced than that presented in this work.

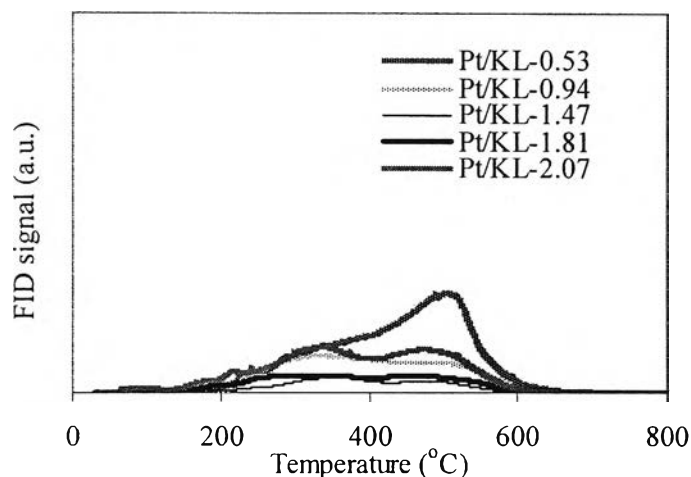


Figure 4.12 TPO profiles of coke deposits left over the different catalysts after 550 min time on stream during n-octane aromatization. Reaction conditions: Temperature= 500°C, WHSV= 5 h⁻¹, and H₂/HC= 6.

4.5 Conclusions

It has been shown that during the synthesis of KL zeolite by the microwave thermal method, parameters such as ageing time, amount of Ba and amount of seeding have an important effect on the resulting zeolite particle size. It was found that small crystallites can be obtained using long ageing times and the larger amounts of seeding material in the range of 2-5 wt%. The degree of zeolite crystallinity is greatly improved by the addition of Ba, but at the same time the size of the zeolite crystallite increases with increasing amounts of Ba

Regarding the catalytic performance, it was found that the crystal size had a great effect on the observed EB/OX ratio. The larger particle size gave the higher EB/OX ratio due to an enhanced restriction to the diffusion of OX through the zeolite channels. In order to maximize C8-aromatics by avoiding secondary hydrogenolysis, zeolites with shorter pore length are required.

4.6 Acknowledgements

This work was supported by the Thailand Research Fund (TRF), the Petroleum and Petrochemical Technology Consortium (PPT) through CU-PPC of the Petroleum and Petrochemical College, Chulalongkorn University, and Ratchadapiseksomphot Endowment Fund of Chulalongkorn University. We gratefully acknowledge Oklahoma Center for Advancement of Science and Technology (OCAST) for providing financial support of the work accomplished at the University of Oklahoma.

4.7 References

1. Meriaudeau, P. and Naccache, C., (1997). *Catal. Rev.-Sci. Eng.*, 39, 5-48.
2. Bernard, J.R. (1980). *Proceedings of the Fifth International Conference on Zeolites*, L.V.C. Ress (Ed), Heyden, London, 686.
3. Hunges, T.R., Buss, W.C., Tamm, P.W. and Jacobson, R.L., *Stud. Surf. Sci Catal.* (1986), 28, 725-732.
4. Tamm, P.W., Mohr, D.H. and Wilson, C.R., *Stud. Surf. Sci. Catal.* (1988), 38, 335-353.
5. Jacobs, G., Ghadiali, F., Pisano, A., Borgna, A., Alvarez, W.E. and Resasco, D.E. (1999). *Appl. Catal. A*, 188, 79-98.
6. Jacobs, G., Alvarez, W.E. and Resasco, D.E. (2001). *Appl. Catal. A*, 206, 267-282.
7. Jongpatiwut, S., Sackamduang, P., Osuwan, S., Rirksomboon, T. and Resasco, D.E. (2003). *J. Catal.*, 218, 1-11.
8. Treacy, M.M.J. (1999). *Micropor. Mesopor. Mater.*, 28, 271-292.
9. Verduijn, J.P., Mertens, M.M. and Antanis, M.H. (2001). *US Pat. 6 258 991 B1*.
10. Break, W.N. and Nancy, A. (1965). *US Pat. 3 216 789*.
11. Wortel, T.M. (1985). *US Pat. 4 544 539*.
12. Verduijn, J.P. (1987). *Eur. Pat. Appl. 219 354*.
13. Verduijn, J.P. (1991). *Int. Pat. WO 91/06367*.

16. Park, M. and Komarneni, S. (1998). *Micropor. Mesopor. Mater.*, 20, 39-44.
17. Romero, M.D., Gomez, J.M., Ovejero, C. and Rodringuez, A. (2004). *Mater. Res. Bull.*, 39, 389-400.
18. Renzo, D.F. (1998). *Catalysis Today*, 41, 37-40.
19. Gontier, S. and Tuel, A. (1996). *Zeolites*, 16, 184-195.
20. Qinghua, L., Mihailova, B., Creaser, D. and Sterte, J. (2001). *Micropor. Mesopor. Mater.*, 43, 51-59.
21. Parrillo, D.J., Adamo, A.T., Kokotailo, G.T. and Gorte, R. J, (1990) *Appl. Catal.*, 67, 107-118.
22. Slangen, P.M., Jansen, J.C. and Beckhum, H.V. (1997). *Microporous Mater.*, 9, 259-265.
23. Joshi, P.N., Kotasthane, A.N. and Shiralkar, V.P. (1990). *Zeolites*, 10, 598-602.
24. Ertl, G., Knozinger, H. and Weitkamp, J. (1997). *Handbook of Heterogeneous Catalysis*, VCH Press, Germany.
25. Hincapie, B.O., Garces, L.J., Ahang, Q., Sacco, A. and Suib, S.L. (2004). *Micropor. Mesopor. Mater.*, 67, 19-26.
26. Davis, R.J. (1994). *HCR Concise Review*, 41-53.
27. Jongpatiwut, S., Trakarnroek, S., Rirksomboon, T., Osuwan, S. and Resasco, D.E. (2005). *Catal. Lett.*, 100 (1-2), 7-15.